

Article

Investigation of Interfacial Characteristics as a Key Aspect of the Justification of the Reagent Regime for Coal Flotation

Tatyana N. Aleksandrova , Valentin V. Kuznetsov *  and Evgeniya O. Prokhorova 

Mineral Processing Department, Empress Catherine II Saint Petersburg Mining University,
199106 St. Petersburg, Russia; aleksandrova_tn@pers.spmi.ru (T.N.A.); s225074@stud.spmi.ru (E.O.P.)

* Correspondence: kuznetsov_vv@pers.spmi.ru

Abstract: This work presents a comprehensive approach for the justification of the reagent regime of coal flotation by investigating the interfacial characteristics of flotation phases with various techniques. For the energy characterization of the surface processes in flotation systems, a method of establishing the components of the specific surface Gibbs energy on the basis of a numerical estimation of surface free energy change during the adsorption of flotation reagents using the Owens–Wendt–Rabel–Kaelble technique was proposed. Using the developed approach, the features of the kinetics of n-hexane sorption on the surface of coal samples were established. The substantiation of differences in the potential mechanisms of the fixation of strictly apolar and aromatic reagents is based on the results of the quantum–chemical modeling of the states of the coal–adsorbate system using the software packages Avogadro and Orca. The simulation shows the possibility of aliphatic and aromatic reagents’ synergetic effects on coal surface hydrophobization. Based on the results of quantum–chemical modeling, it was found that for the physical adsorption of an oxyethylated nonyl-phenol molecule on a molecular fragment of the coal surface, according to the Weiser model, the decrease in the energy of the system was 0.05562 eV, which indicates the high thermodynamic probability of the physical sorption of this compound. The parameters of the Langmuir monomolecular model for the sorption of oxyethylated nonyl-phenol on the surface of the studied coal samples were established. The criterion characterizing the interphase phenomena in the flotation system based on the results of potentiometric studies of the interfacial characteristics, E_f , was proposed. It was found that for the studied values of the flow rate of oxyethylated nonyl-phenol, the highest value of E_f was achieved when the value of the sorption of the reagent equaled 63.99% of the limiting sorption capacity. The performance of the proposed reagents for coal flotation was confirmed by flotation tests.



Academic Editors: Liuyang Dong,
Peilun Shen, Jia Tian and Ya Gao

Received: 13 December 2024

Revised: 9 January 2025

Accepted: 10 January 2025

Published: 14 January 2025

Citation: Aleksandrova, T.N.;
Kuznetsov, V.V.; Prokhorova, E.O.
Investigation of Interfacial
Characteristics as a Key Aspect of the
Justification of the Reagent Regime for
Coal Flotation. *Minerals* **2025**, *15*, 76.
[https://doi.org/10.3390/
min15010076](https://doi.org/10.3390/min15010076)

Copyright: © 2025 by the authors.
Licensee MDPI, Basel, Switzerland.
This article is an open access article
distributed under the terms and
conditions of the Creative Commons
Attribution (CC BY) license
([https://creativecommons.org/
licenses/by/4.0/](https://creativecommons.org/licenses/by/4.0/)).

Keywords: coal; flotation; surface free energy; molecular modeling

1. Introduction

Today, coal is one of the main strategic resources both in terms of energy generation and raw materials for the chemical and metallurgical industries [1,2]. As of 2022, the share of coal in global energy consumption amounted to 27.2%. Despite the introduction of green energy technologies, coal remains a reliable reserve for providing the world with electricity [3,4]. Such high demand leads to a significant deterioration of coal’s mineral base in terms of initial content and increasing requirements for the use of water, recovery performance, and the environmental safety of its processing [5–7]. The combination of these factors determines the necessity of the coal floatation technologies’ improvement, which

must meet high standards for the performance and ecological compatibility of the process. Such a task must be achieved with the consideration of the elaborate mining, geological, and technological properties of coals [8–10]. Their concomitance can significantly complicate the further processing and utilization of coal raw materials for various purposes [11–13]. All of these factors stipulate the necessity of coal flotation technologies' development, especially in terms of retrofitting the reagent mode as the most flexible part of the flotation process [14,15].

A wide range of works have been devoted to the issues of flotation reagents anchoring on the mineral surface, from the perspective of using the peculiarities of their kinetics to find ways to increase the recovery of valuable components [16–18].

The difficulty in the realization of these approaches in coal flotation lies in the influence of many interrelated factors on the flotation performance, such as the physical and chemical properties of the surface, the presence of functional groups, lattice defects, charges, and the macroscopic properties of phases [19–21]. A possible direction for improving the existing flotation regimes, as well as the justification of fundamentally new flotation reagents for coal preparation, is the development of comprehensive approaches for determining the occurring processes' mechanisms in flotation systems, based both on experimental results [22,23] and the results of computer modeling and the use of neural network technologies to analyze the properties of raw materials [24–26]. In [27], the influence of the interaction mechanism of the microemulsion collector on the enhancement in the low-rank coal flotation was studied by the application of the zeta potential and contact angle measurements for the quantitative characterization of the occurring interfacial processes, and Fourier transform infrared spectroscopy with X-ray photoelectron spectroscopy was utilized for an analysis of the reagent's anchoring onto the mineral surface. In [28], X-ray photoelectron spectroscopy and contact angle measurements were used to indicate the surface properties of candle soot. Scanning electron microscopy with an energy-dispersive spectrometer and an attached time measurer was used to show the adsorption of candle soot on coal particles' surface. A possible way of establishing a link between the results of molecular and kinetic investigation characteristics is calculating the value of surface free surface energy as determined by the ratio of interfacial tension. For example, in [29], for the evaluation of mineral surface hydrophobicity, the parameter of the specific net free energy of the interaction between bubbles and particles immersed in water was introduced. The accessed values were in strong correlation with microflotation recoveries.

Although various parameters for studying the reagents' action on the mineral surface on a molecular level provide exhaustive information on their hydrophobic effects, it is very complicated to scale up these results for practical applications because of the probabilistic nature of flotation. To accomplish this, it is possible to use various kinetic models for flotation processes to correlate the probability of flotation elemental acts with its performance. In [30], a flotation kinetic analysis was used for the validation of the collector dosage reduction possibility via ionic liquid microemulsion application for coal slime. In [31], six flotation kinetics models were implemented to describe the experimental data of coal flotation with nanobubble application.

Therefore, implementing more versatile approaches for studying interfacial characteristics will provide a more definitive understanding of coal flotation mechanisms.

In this paper, a comprehensive approach to the study of surface phenomena in coal flotation on the basis of various techniques for assessing interfacial characteristics is proposed and tested. The goal of this approach is to reveal the ways in which the range of potential reagents' reduction can be achieved and the accuracy of predicting the effectiveness of various reagent regimes can be improved.

2. Materials and Methods

2.1. Characterization of the Research Object

The objects of this study were samples of coal from the Kuznetsk Basin. The elemental composition of the studied samples by size classes, as determined by X-ray fluorescence spectroscopy, is presented in Table 1.

Table 1. Elemental composition of the investigated coal samples.

Size Class, mm	Yield, %	Percentage Ash Content, %	Content, %							
			Si	Fe	S	Al	Ca	K	Ti	Sr
−2 + 0.5	1.41	22.99	3.23	3.29	1.66	0.82	1.58	1.69	0.53	0.07
−0.5 + 0.25	37.98	22.99	2.91	3.63	1.73	0.53	2.08	1.47	0.49	0.12
−0.25 + 0.16	18.64	27.81	3.32	3.77	1.93	0.90	3.09	1.78	0.64	0.21
−0.16 + 0.071	19.16	29.16	3.02	3.53	1.45	0.71	4.70	2.03	0.59	0.36
−0.071	22.82	40.74	5.80	4.98	1.15	1.14	5.88	2.87	0.63	0.81
Summary	100.00	29.12	3.67	3.94	1.58	0.78	3.63	1.96	0.57	0.34

Based on the obtained results’ analysis, it is established that the lowest content of organic part is characteristic of the sieve class −0.071 mm. Based on the contents of Si, Fe, and Al, it is also confirmed that the finest class is the most abundant in minerals of the host rock. At the same time, the redistribution of sulfur in classes with lower ash content indicates that sulfur is largely associated with the organic part.

To determine the density properties of the coal sample under study, densimetric analysis was performed using calcium chloride solution. In changing the concentration of the solution, the density also changed, which resulted in the material with lower density floating and being weighed as a separate density fraction. The calcium chloride solution concentration varied in range from 2% to 34%. The density of solution was measured by the areometer. The coal began to float at a solution density equal to 1240 kg/sm³. Fractions were separated at the following values of the solution’s density: 1270 kg/sm³, 1286 kg/sm³, 1295 kg/sm³, and 1309 kg/sm³. At a density of 1320 kg/sm³, all the material was emersed. The results of densimetric analysis are shown in Figure 1.

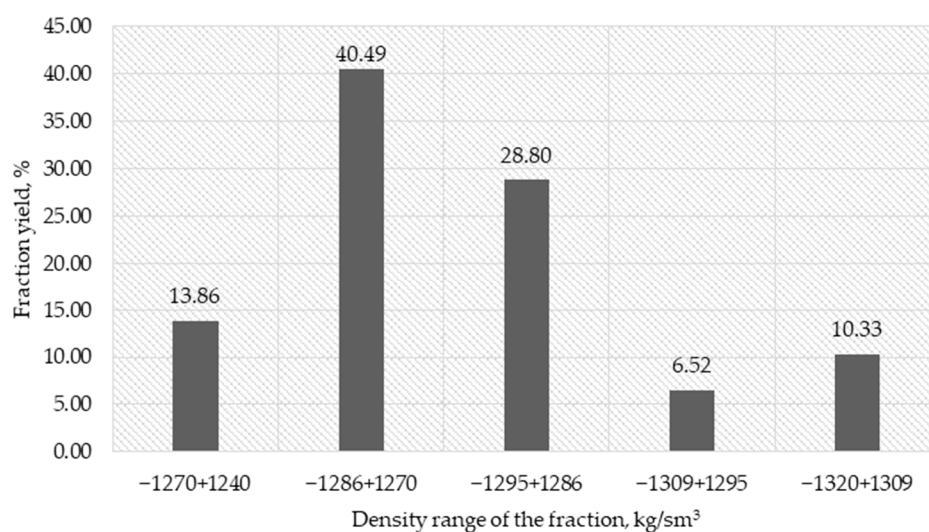


Figure 1. Results of the densimetric analysis.

According to the results of the data analysis in Figure 2, it is established that the coal particles in the studied sample have density values that are in the range of 1270 kg/sm³ to

1320 kg/sm³. More than 80% of the particles in the sample have density value less than 1295 kg/sm³. The fraction with a density range of 1270 kg/sm³ to 1286 kg/sm³ has the highest yield value. The dominance of denser particles in the sample is probably due to the fine inclusions of rock minerals, which determine the ash content of the sample. According to the density characteristics, the studied coal samples can be categorized into the vitrinite group. This type of coal belongs to the shiny variety characterized by a low degree of metamorphism and a high content of aromatic compounds.

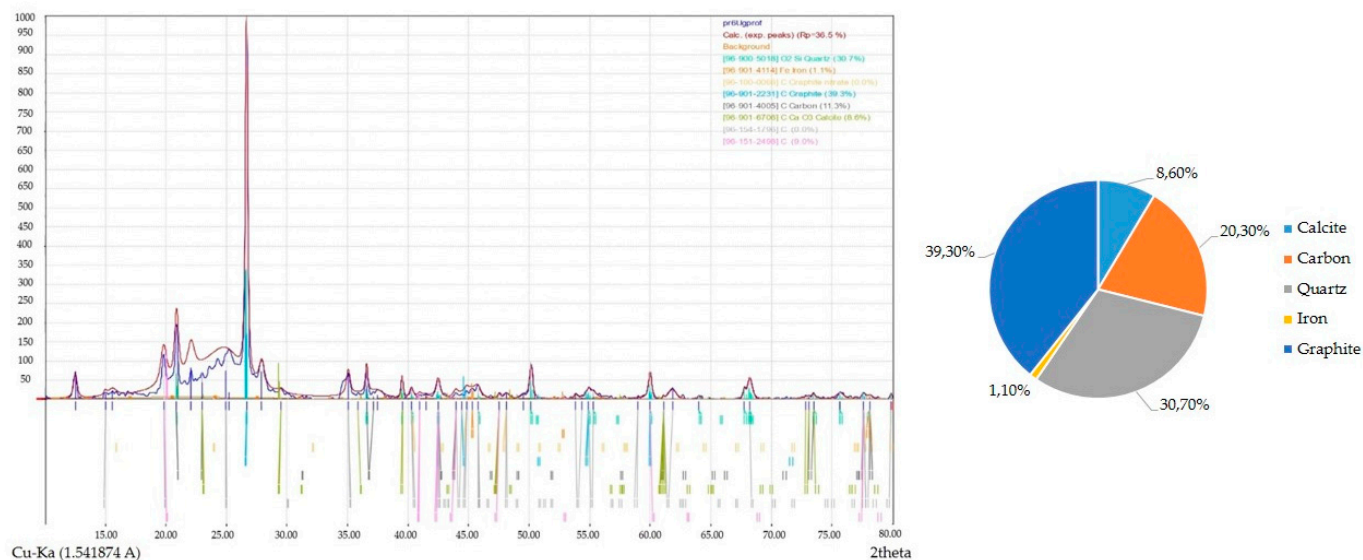


Figure 2. X-ray diffraction results of the studied coal samples.

The composition of rock minerals was analyzed by the X-ray diffractometry method. Experiments on X-ray diffraction for obtaining information on the structural properties of minerals were carried out using Shimadzu X-ray powder diffraction equipment. The sample, preliminarily grinded to 20 microns, was placed in a cuvette of 700 mg and tightly compressed in the form of a tablet. The results of the studies are presented in Figure 2.

Based on the obtained results, it is established that the predominant gangue minerals are calcite and quartz.

2.2. Methodology of Quantum–Chemical Modeling of the Process of Reagent Anchoring

The differences in the potential mechanisms of the reagents anchoring on the mineral surface during flotation were substantiated based on the results of quantum–chemical modeling of the states of the mineral–adsorbate system using the software packages Avogadro and Orca 5.0 [32–34].

Optimization of the molecule structure was carried out by using the universal force field (UFF) method. The essence of this method is to represent the sum of potential energies from changes in all geometrical parameters of a molecule or molecular system as the total potential energy of the molecular system (superposition of all acting force fields). Through the performance of various iterations of molecular geometrical parameters, the smallest possible value of total potential energy is determined, which corresponds to the most stable form of the molecule.

After geometric optimization of the molecule, the potential co-state of the system surface under study—water—is modeled to determine the free energy of the surface. For this purpose, the Conductor-like Polarizable Continuum Model (CPCM) method, based on the electron density functional theory, is used. The simplified algorithm of the method is presented in Figure 3.

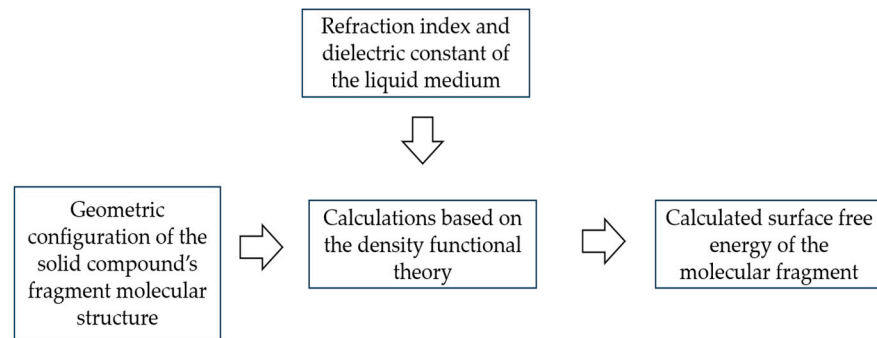


Figure 3. CPCM method for surface free energy calculation [35,36].

In this model, water is considered as a solvent with properties identical to those of a conductor-like polarizable medium, and the main parameters of the method are the refractive index and dielectric constant of the medium. In this model, the molecule under study is placed in an abstract cavity, the walls of which are represented by a solvent. The solvent is represented by a continuous medium that interacts with the charges on the surface of the molecule. Thus, an electron density function describing the contact between the solvent and the molecule is constructed, from which the value of the specific surface energy can be derived. After that, the method is repeated, but for the case where reagent is adsorbed on the mineral surface. Modeling is performed near the nodes of molecules with the main functional groups with placement near water molecules. After the system energy minimization procedure, molecules of potential apolar collectors are added to the system (in case of the present study—*n*-hexane and phenol). The obtained results of the surface energy are then averaged [35,36].

According to the results of quantum–chemical modeling, the parameters of the structural molecule of coal are determined, and the values of the theoretical free energy of the surface and the free energy of the surface at adsorption of the reagent are determined using density functional methods. After that, the values of parameters of chemical models are corrected, taking into account the results of experimental studies of surface free energy.

2.3. Methodology for Numerical Determination of the Surface Free Energy Value Using the Owens–Wendt–Rabel–Kaelble Method

Numerical determination of surface free energy changes is possible through the determination of surface tension at the liquid–solid–gas interface. In order to quantify the surface free energy value and its components, we measured contact angles at the mineral–liquid–air interface for water and 52% Na_2CO_3 solution. When using two liquids that differ in chemical composition and structure, it is possible to establish the ratio of surface energy components due to different categories of interfacial interactions. Numerically, they will be equal to the change in surface tension at the liquid–solid interface. In this work, the Owens–Wendt–Rabel–Kaelble (OWRK) method was applied for the determination the ratio of surface free energy components. The numerical values of the surface tension components are determined from the solution of the system of equations [37]:

$$\begin{cases} \frac{\sigma_{L1}(\cos\theta_1+1)}{2\sqrt{\sigma_{L1}^D}} = \frac{\sqrt{\sigma_s^P}\sqrt{\sigma_{L1}^P}}{\sqrt{\sigma_{L1}^D}} + \sqrt{\sigma_s^D} \\ \frac{\sigma_{L2}(\cos\theta_2+1)}{2\sqrt{\sigma_{L2}^D}} = \frac{\sqrt{\sigma_s^P}\sqrt{\sigma_{L2}^P}}{\sqrt{\sigma_{L2}^D}} + \sqrt{\sigma_s^D} \end{cases} \quad (1)$$

where σ_{L1} , σ_{L2} are the values of surface tension of liquids used for analysis, at the air–liquid interface; σ_{L1}^P , σ_{L2}^P are the values of polar components of surface tension of liquids used for analysis, at the air–liquid interface; σ_{L1}^D , σ_{L2}^D are the values of the dispersive components of

the surface tension of the liquids used for analysis, at the air–liquid interface; σ_S^D , σ_S^P are the values of dispersive and polar components of the free energy of the mineral surface, respectively; and $\cos\theta_1$, $\cos\theta_2$ are the contact angles for the first and second analyzed liquid.

2.4. Methodology for Potentiometric Determination of Interfacial Characteristics at the Solid–Liquid–Gas Interface

This method is based on the occurrence of electrostatic potential when particles settle, known as sedimentation potential [38,39]. However, in this case, the potential appears because of the organized movement of the solid and gas phases in a column full of liquid. The scheme of the installation is presented in Figure 4. Two electrodes made of titanium alloy and are placed in a water column. The height of the column is 35.5 cm. The length of the electrodes is 20.5 cm. The diameter of the electrodes is 0.8 cm. The ends of the electrodes are placed at different heights. The height difference is 5 cm. A voltmeter is connected to the ends of the electrodes in the air by terminals to record the values of the resulting potential difference. The bottom of the column is connected to the air supply tube, which is connected to an air compressor. The air compressor should provide an airflow rate of at least 0.5 l/min. The height of the compressor should be higher than the top edge of the column. At the bottom of the column, a plastic grid with a sieve mesh diameter of 0.5 cm is installed to ensure the dispersion of the supplied air.

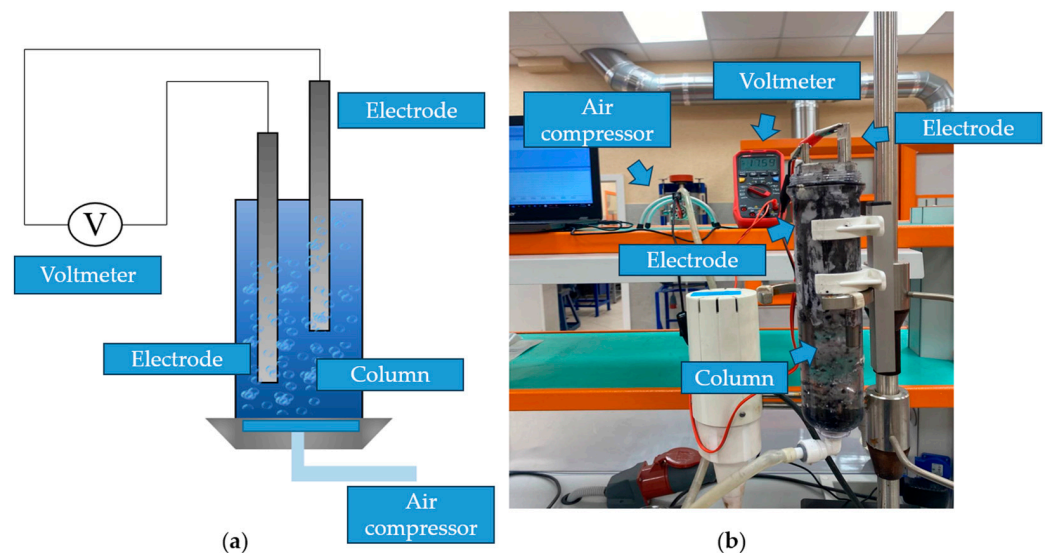


Figure 4. Setup for potentiometric determination of interfacial characteristics in coal flotation ((a)—setup scheme, (b)—photo of the setup).

To determine the interfacial characteristics for the gas–liquid system, 150 mL of distilled water is poured into the column. Afterwards, the air supply is switched on and the values of the resulting potential difference are recorded on a voltmeter for at least 10 min.

To determine the interfacial characteristics for the solid–liquid–gas system, a sample of the material under study is first taken based on the required value of the solid content for flotation separation. A selected sample is placed in the reactor, and the volume of the mixture is brought to 150 mL with distilled water and stirred for 5 to 10 min. After loading the suspension into the column, the air supply is switched on, and the values of the resulting potential difference are recorded on a voltmeter for at least 10 min. The potential difference starts to be recorded starting from 30 s after the air supply. The obtained values are interpreted using the following equation:

$$U = E_f \ln(t) + C, \quad (2)$$

where U is the fixed value of arising potential difference, V ; t is the analysis time, s ; E_f is the coefficient characterizing interphase phenomena in the flotation system, V/s ; and C is the correction factor taking into account the background due to the ionic composition of the medium.

The prepared sample must be preliminarily crushed or grinded. The size of the particles in the analyzable sample must be less than 2 mm. The mass of the sample must be less than 10 g.

2.5. Flotation Tests

Flotation experiments were carried out with the use of a pneumomechanical flotation machine, a Flotation Bench Test Machine (Laarmann Group B.V., Roermond, The Netherlands), with a chamber volume of 1.5 l. The solid content varied in the range of 20–25%. Preparation included preliminarily grinding the sample to a size of less than 500 μm . As a depressor, a blend of sodium pyrophosphate and sodium silicate was used with a fixed consumption rate of 200 g/t. As a collector, an emulsion of spindle oil and oxyethylated nonyl-phenol was used based on the theoretical research results. The consumption rate varied from 500 g/t to 1500 g/t.

3. Results and Discussion

3.1. Investigation of the Mechanism of Action of Flotation Reagents Based on the Estimation of the Free Energy of the Surface of Minerals

The action of the collector in flotation is mainly derived from its adsorption on the mineral surface which therefore hydrophobizes it, which allows the mineral particle to attach to the surface of the air bubble. The hydrophobization effect caused by the presence of apolar fragments in the collector (or the collector itself is fully apolar), which cause an increase in the required work of adhesion for water due to differences in polar moment. In this case, the collector affects the change in the probability of flotation recovery of the mineral aggregate in two ways:

- A change in the probability of the collision of a mineral aggregate with an air bubble due to a decrease in the energy of the hydrate barrier of water molecules at the mineral–liquid interface;
- A change in the probability of maintaining the mineral particle–air bubble contact by increasing the required work of adhesion for water.

The value of this energy can be quantitatively evaluated as a change in the surface free energy ($\text{SFE} - E_s$), which consists of two components: dispersion and polar. The first component includes orientation, induction, and dispersion interactions due to the difference in the dipole moments of the interacting substances of the phases [40–42]. Those interactions in flotation are mainly presented by the physisorption of reagents on the surface and the contact of the bubble and hydrophobic mineral surface. The second component combines the interactions caused by the formation of hydrogen bonds, charge transfer, and the formation of chemical bonds. The polar component in flotation mainly shows the potential of chemisorption and, in the case of the mineral surface, the amount of energy that can be used for creating the barrier of the water molecules [43].

In the case of the application of apolar collectors, which are characteristic of coal flotation, the physical form of reagent sorption will prevail. The peculiarity of this type of sorption is multilayer in contrast to chemisorption. Due to the intermolecular forces of interaction, it is possible to form a second layer of collector molecules.

From the position of the second law of thermodynamics, the occurring processes of reagent fixation can be described as changes in surface energies at the phase boundary.

The energy of the system before contact can be described by the following equation:

$$E_1 = E_{s1} + E_{w-g} + E_{w-c}, \quad (3)$$

where E_{s1} is the free energy of the solid surface before contact, J; E_{w-g} is the energy of the water–gas interface, J; and E_{w-c} is the energy of the water–gas interface, J.

The energy of the system after contact can be described by the following equation.

The change in the energy of the system during adsorption will be equal to

$$\Delta E = E_2 - E_1 = E_{s2} - (E_{s1} + E_{w-g} + E_{w-c}), \quad (4)$$

The process will proceed spontaneously at $\Delta E < 0$. The peculiarity of determining the free energy of the surface using the OWRK method is that the surface tension at the solid–liquid interface, which is its measure, indicates the amount of energy that the surface can expend to form new bonds. Thus, when measuring the SFE before and after the reagent anchoring on the surface, it is possible to estimate the energy spent on the formation of new bonds on the solid surface as a difference of the following potentials:

$$E_{s2} - E_{s1} = \sigma_{s1} - \sigma_{s2}, \quad (5)$$

The energy change in the system can be considered the specific value of the Gibbs energy per elementary area of interfacial contact:

$$\frac{\partial G}{\partial S} = \Delta G_s = \sigma_{s1} - \sigma_{s2} - \sigma_{w-g} - \sigma_c, \quad (6)$$

where σ_{s2} is the specific free energy of the solid surface after contact, J/m², σ_{s1} is the specific free energy of the solid surface before contact, J/m²; σ_{w-g} is the specific energy of the water–gas interface, J/m²; and σ_c is the specific energy of the water–collector interface, J/m². A graphical interpretation of the calculation of the specific Gibbs energy algorithm is presented in Figure 5.

Evaluation of the values of the change in the polar and dispersive components of the specific Gibbs energy will allow us to judge the mechanism of hydrophobization and hydrophilization of the mineral surface during coal flotation. Based on the relationship (5), they can be calculated by the following equations:

$$\Delta G_s^D = \Delta \sigma_S^D - \sigma_c - \sigma_{w-g}^D, \quad (7)$$

$$\Delta G_s^P = \Delta \sigma_S^P - \sigma_{w-g}^P, \quad (8)$$

In this work, with the use of the OWRK methodology, we experimentally determined the changes in the values of SFE components of the studied coal samples without surface treatment and with treatment with n-hexane.

For the untreated surface of the coal, the following values of SFE and its components were determined: $\sigma_{s1} = 43.81$ mJ/m², $\sigma_{s1}^D = 40.09$ mJ/m², and $\sigma_{s1}^P = 3.71$ mJ/m². The results of calculation of the SFE and its components, based on the results of measurements of the contact angles of the analyzed liquids on the coal surface as a function of the contact time of n-hexane with the coal surface via Equation (1), are shown in Figure 6.

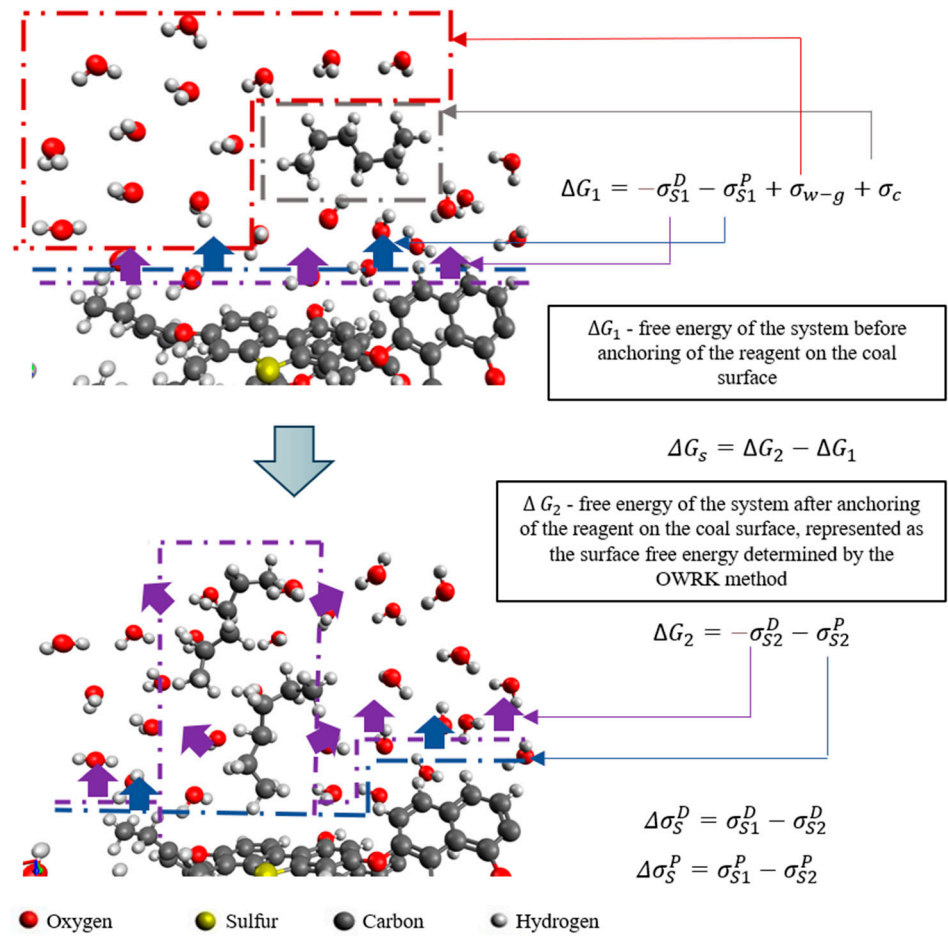


Figure 5. Graphical interpretation of the calculation of the value of specific Gibbs energy of surface phenomena.

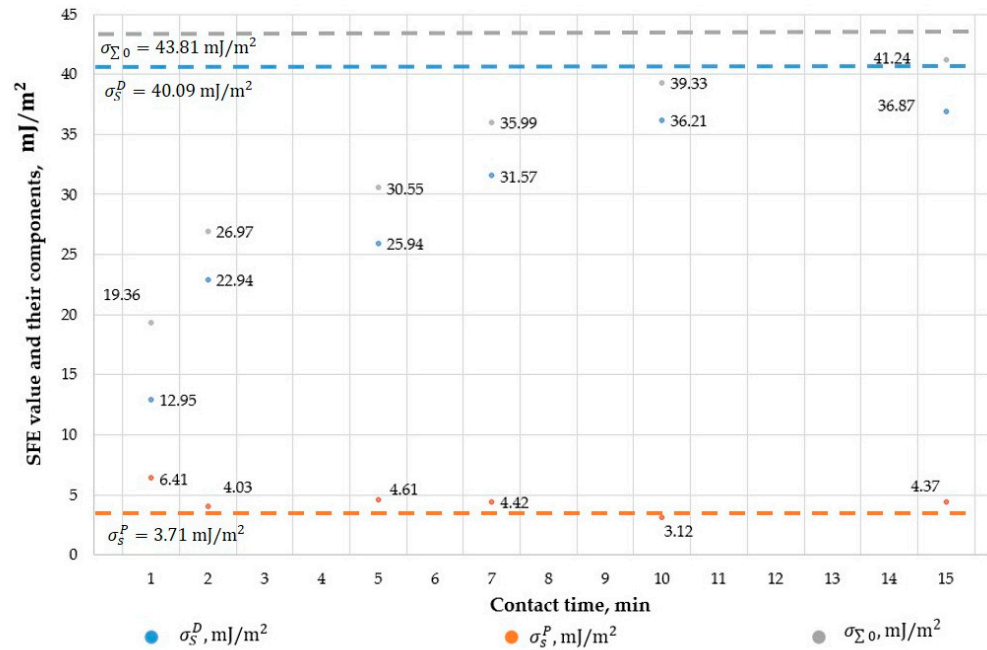


Figure 6. Dependence of the SFE values on the sample holding time in the reagent.

Based on the analysis of the data in Figure 1, it was found that with increasing exposure time, the values of SFE and its dispersive component increase according to the step law, while the polar component decreases and from 2 min fluctuates in the range

of 3.0–4.5 N/m. The minimum value of the polar component is reached at a processing time of 10 min. The increase in the SFE values is probably due to the formation of apolar reagent microdroplets on the coal surface, which have their higher potential to form bonds of electrostatic nature, which is also confirmed by the growth of the dispersion component. This energy is transferred from the energy potential of the collector–water interface.

The calculations of polar and dispersion components of ΔG_s via Equations (6) and (7) are summarized in Table 2.

Table 2. Results of surface free Gibbs energy.

Contact Time, min	ΔG_s^D , mJ/m ²	ΔG_s^P , mJ/m ²	ΔG_s , mJ/m ²
Without treatment	-	-	-
1	-13.08	-53.70	-66.78
2	-23.07	-51.32	-74.39
5	-26.07	-51.90	-77.97
7	-31.70	-51.71	-83.41
10	-36.34	-50.41	-86.75
15	-37.00	-51.66	-88.66

Based on the analysis of the data in Table 1, it was found that the value of specific Gibbs energy decreases with increasing contact time. The lowest value of specific Gibbs energy indicates the highest probability of the process. The decrease in this value with time indicates an increase in the probability of sorption of the reagent on the surface, since the formation of new bonds of the reagent with the surface is energetically less costly. It is also found that the value of the dispersive component of the specific Gibbs energy decreases with increasing contact time, indicating that the sorption of the reagent occurs predominantly due to the physical form of sorption. The decrease in the loss of ΔG_s^D value with time indicates that the more n-hexane is sorbed on the surface, the less available area remains for subsequent sorption steps. When full filling is reached, the reagent molecules will be able to be retained near the surface only due to the polylayer adsorption caused by the intermolecular interaction of the sorbing molecules.

Based on this, it is possible to judge the mechanism of fixation of the collector on the basis of the ratio of the components of the dispersion component of the specific Gibbs energy.

When the condition of

$$|\Delta G_s^D| < \sigma_c + \sigma_{w-g}^D$$

is met, the surface potential for the formation of dispersion bonds with the collector is not completely used up. The decrease in the Gibbs energy is caused by monomolecular adsorption of apolar collector on the mineral surface.

When the condition of

$$|\Delta G_s^D| > \sigma_c + \sigma_{w-g}^D$$

is met, the surface potential for the formation of dispersion bonds with the collector is completely wasted. The decrease in the Gibbs energy is due to the formation of multi-layer adsorption structures of the apolar collector and their potential for the formation of dispersion bonds.

A similar logic can be applied to the case of fixation of the depressor on the surface of rock-forming minerals. One of the hydrophilizing effects of the depressor is the formation of a powerful hydrate barrier surrounding the mineral surface.

When the condition of

$$|\Delta G_s^P| < \sigma_{w-g}^P$$

is met, the surface potential for the formation of polar bonds with the reagent is not used up completely. The decrease in Gibbs energy is due to adsorption of the depressor on the mineral surface.

When the following condition is met:

$$|\Delta G_s^P| > \sigma_{w-g}^P$$

The surface potential for the formation of polar bonds with the reagent is completely spent. The decrease in Gibbs energy is due to the formation of hydrate layers and their potential for the formation of polar bonds.

3.2. Predicting the Efficiency of Fixation of Reagent Molecules on the Coal Surface Using Quantum–Chemical Modeling

Based on the results of the analysis of the elemental composition and physicochemical properties of the studied coal samples, the Weiser model (Figure 7) was chosen to build a structural model of the elementary unit of the molecular structure of coal [44,45].

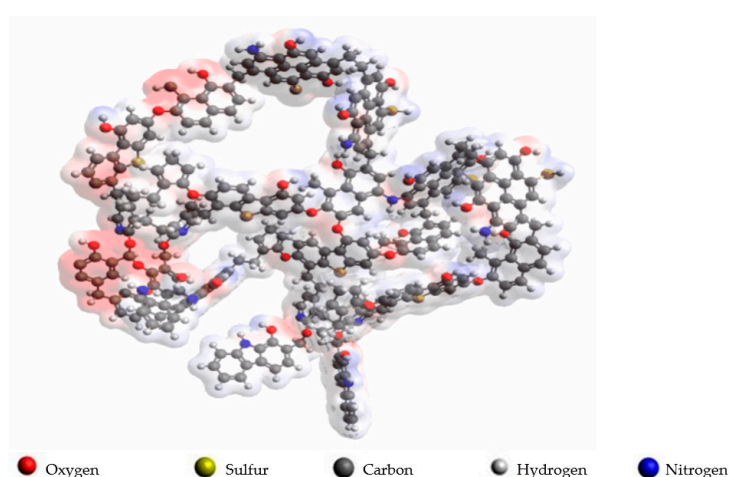


Figure 7. Visualization of the calculation of the specific surface energy of coal using the Weiser structural model with solvent, using the CPCM method based on the electron density function.

The predicted values of predicted surface free energy upon contact with water were established for the predicted Weiser structure of the elementary unit structure of the coal molecule. In addition, these parameters were predicted at possible fixation by the mechanism of physical adsorption for separate molecules of n-hexane (Figure 8) and phenol and their joint fixation at a molar ratio of 1:1.

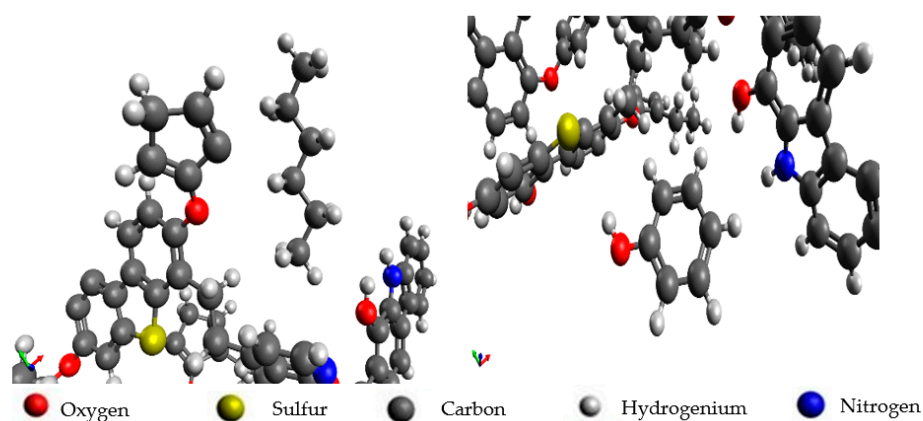


Figure 8. Visualization of the attachment of n-hexane and phenol molecules on the elemental structural unit of a coal molecule.

The determined values of the predicted contact energy and free energy of the system and its changes are shown in Figure 9.

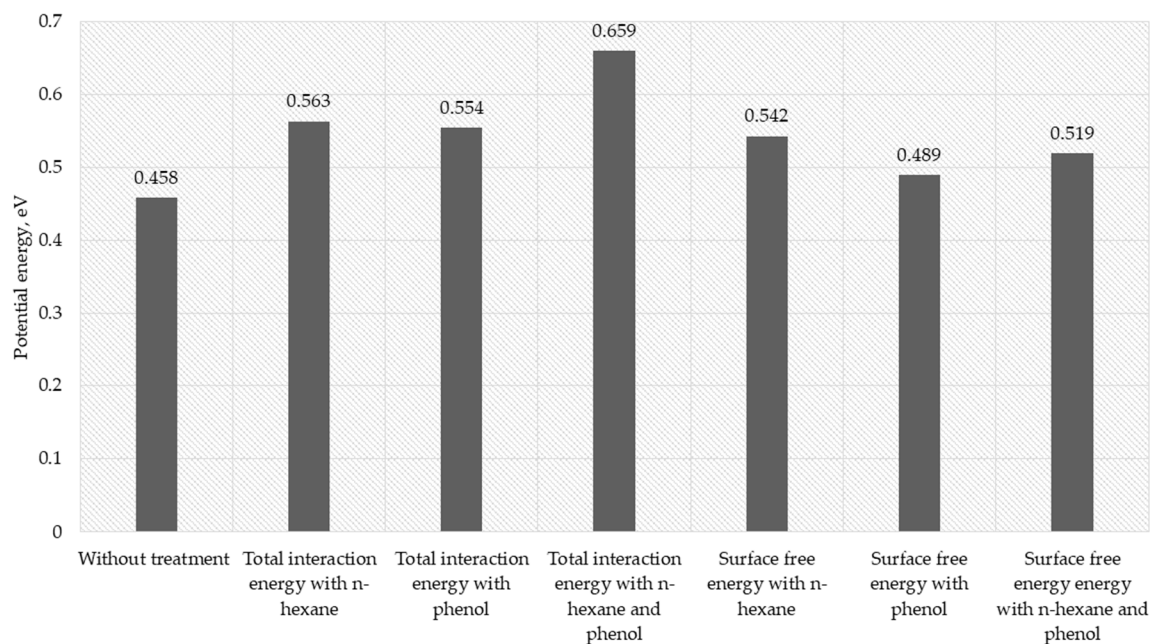


Figure 9. Values of potential energy of systems during the adsorption of reactant molecules on the coal surface.

For the successful adsorption of a molecule on coal surface, it is necessary that the energy of the system decreases in comparison with the initial values of the individual systems. Thus, the greater the difference between the free energy of the system and the potential energy of the systems of coal molecules and reagents (i.e., the lowering of the energy of the system), the more efficient and probable the adsorption process of the reagent. The estimation of the decrease in energy during adsorption is shown in Figure 10.

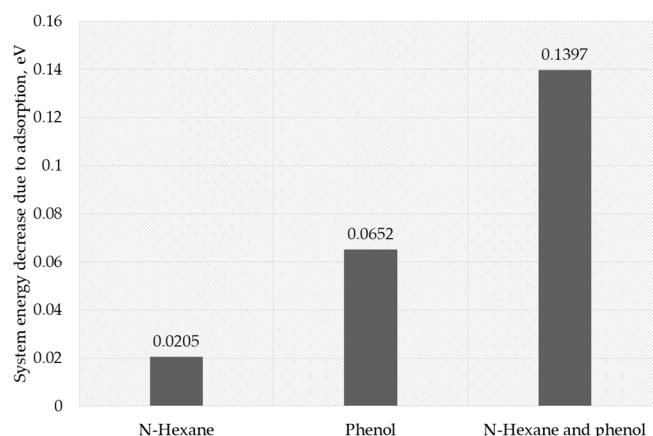


Figure 10. Values of the reduction in potential energy of systems upon adsorption of reagent molecules on the coal surface.

Based on the analysis of the data in the figure, it was found that the largest value of energy decrease in the system is predicted upon simultaneous adsorption of n-hexane and phenol on the coal surface. The predicted value is 0.07448 eV higher than for adsorption of phenol only and 0.01192 eV higher than for adsorption of the n-hexane molecule only.

Thus, the simulation shows the possibility of the synergistic effect of hydrophobization of the coal surface by reagents consisting of both purely apolar compounds and compounds

with a relatively heteropolar structure. The energy decrease in the system upon adsorption of n-hexane and phenol simultaneously has a non-additive character.

On the basis of the obtained results, an oxyethylated nonylphenol that contains both a phenol functional group and an alkyl radical has been selected for further analysis (Figure 11).

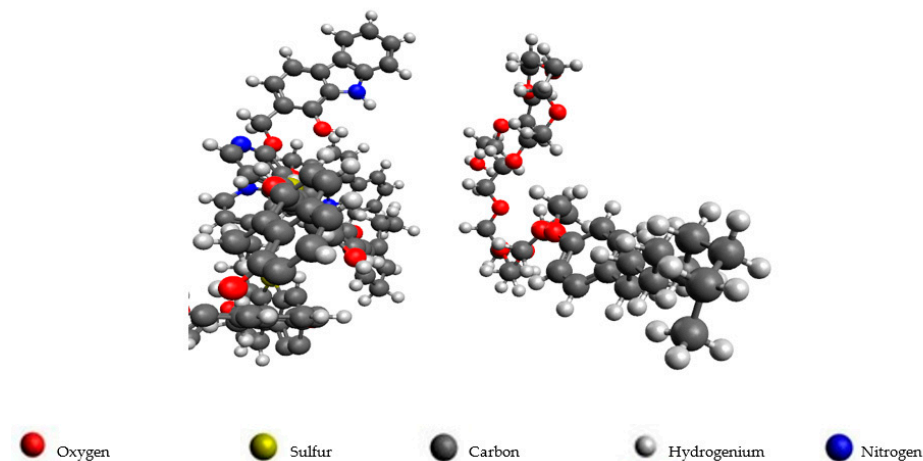


Figure 11. Visualization of the anchoring of an oxyethylated nonyl-phenol molecule on an elementary structural unit of a charcoal molecule according to the Weiser model.

Based on the results of quantum–chemical modeling, it was found that for physical adsorption of oxyethylated nonyl-phenol molecule on the molecular fragment of the coal surface according to the Weiser model, the decrease in the energy of the system was 0.05562 eV, which indicates a high thermodynamic probability of physical sorption of this compound.

3.3. Potentiometric Studies of Interfacial Characteristics in the Coal Flotation Process

The studied reagent was used for further studies of interfacial characteristics using potentiometry of sedimentation potential. The preliminary parameters of the Langmuir monomolecular model for sorption of oxyethylated nonyl-phenol on the surface of the studied coal samples for solutions of the reagent of different molar concentrations were established. The results are presented in Figure 12. The parameters of the Langmuir monomolecular adsorption equation were established as follows (8):

$$\Gamma = 3.206 \frac{\text{mol}}{\text{kg}} \cdot \left(10.59 \cdot \frac{C_m}{1 + 10.59 C_m} \right) \quad (9)$$

where C_m is the molar concentration of the reagent in pulp, mol/L, and Γ is the model reagent sorption value, mol/kg.

Based on the obtained dependence, the limiting sorption capacity for the studied coal samples is 3.206 mol/kg. The obtained model was used to calculate the value of adsorption of the reagent, achieved at the maximum value of the hydrophobization criterion, which allowed us to establish the reagent flow rate at which these conditions of hydrophobization can be achieved.

The determination coefficient of the model totaled 0.9673, which shows the high adequacy of the prediction equation.

For potentiometric studies of interfacial characteristics, a 10 g sample weight of coal was taken. The determined values of the E_f parameter for different systems and reagent regimes were compared with each other. The greater the absolute change in the E_f parameter

compared to the value obtained for the water–air–solid system, the more effective the flotation separation (Table 3).

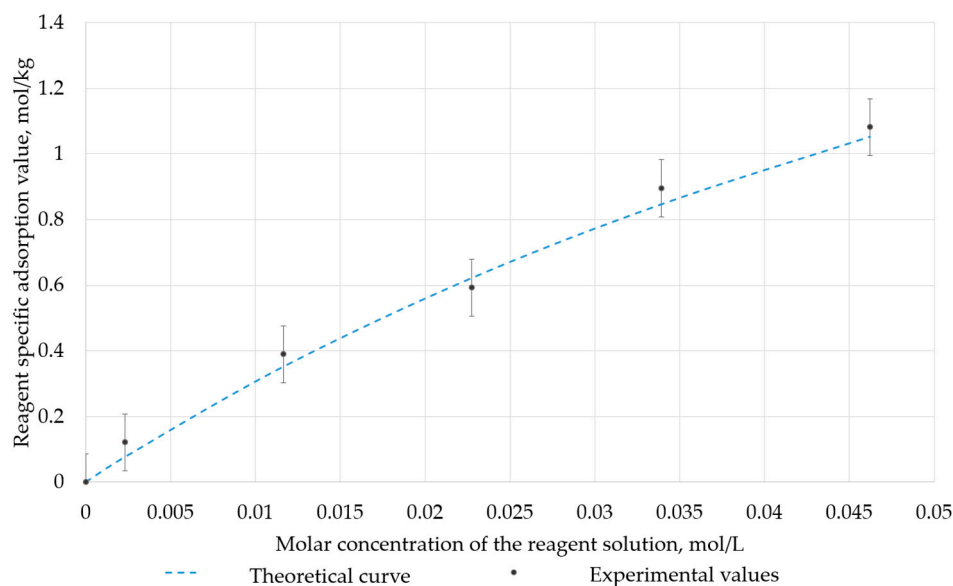


Figure 12. Dependence of the value of specific adsorption of oxyethylated nonyl-phenol as a function of the molar concentration of the reagent in solution.

Table 3. Results of determination via the potentiometric method of interfacial characteristics during coal flotation depending on different reagent flow rates.

Condition	Liquid + Gas	Liquid + Gas + Solid	Liquid + Gas + Solid + Solids + Surfactants			
Reagent flow rate, g/t	0	0	50	150	250	500
Molar concentration of reagent in pulp, mol/L	0	0	0.17	0.50	0.84	1.68
Model reagent sorption value, mol/kg	0	0	2.05	2.70	2.88	3.04
Fraction of sorption from ultimate capacity	0	0	0.64	0.84	0.90	0.95
Parameter E_f , V/s	−0.047	−0.003	7.02	−0.08	−0.01	0.58
Parameter C	0.3928	0.0208	−19.60	19.94	17.68	15.83

According to the results of potentiometric studies of interfacial characteristics, it was found that for the investigated values of the flow rates of oxyethylated nonyl-phenol, the highest value of the criterion E_f is 7.023 V/s. In accordance with the established parameters of the adsorption model, this value corresponds to the reagent sorption value of 63.99% of the limiting sorption capacity. A further increase in the reagent flow rate led to a decrease in the parameter E_f , which is probably associated with an increase in the recovery of the mineral phase of the host rock in the froth product and, as a consequence, a decrease in the selectivity of the flotation enrichment of coal.

3.4. Experimental Validation and Testing on Coal Samples

The proposed approach of measuring was tested for the studied coal sample, as well as samples of calcite and quartz monofractions as the main examples of minerals of the host rocks. As collectors, diesel fuel, spindle oil, and kerosene were used as reagents; as host rock depressors, sodium pyrophosphate, sodium silicate, and carboxymethylcellulose

(CMC) were used as reagents. The results of the experimental determination of values of specific Gibbs energy components are presented in Figure 13.

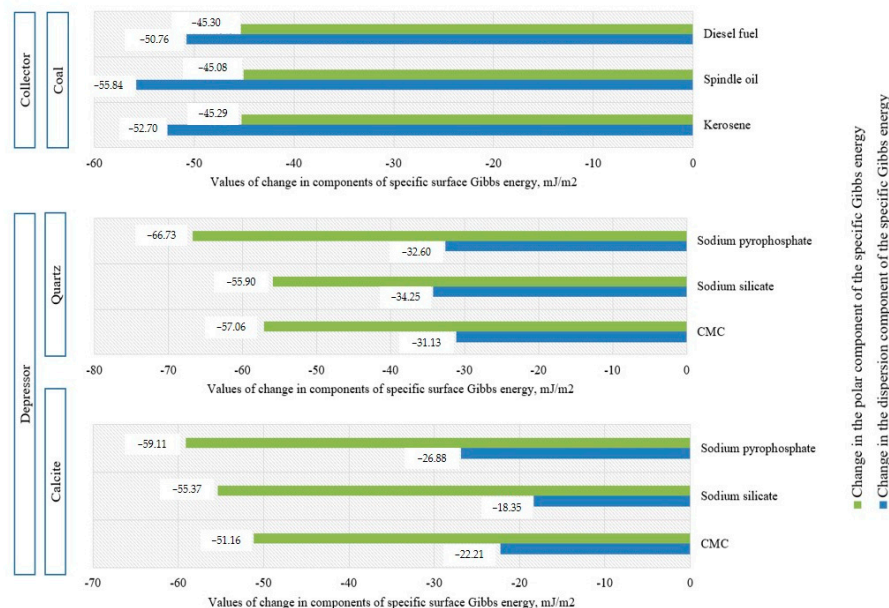


Figure 13. Dependence of the SFE values on the samples’ exposure time in the reagent.

The lower the value of ΔG_s^D , the more effective the hydrophobizing effect of the collector. The lower the value of ΔG_s^P , the more effective the hydrophilizing action of the depressor.

Based on the results obtained, it was found that the highest hydrophilizing effect was achieved by spindle oil against coal. The greatest hydrophilizing effect was established for sodium pyrophosphate in relation to quartz and calcite. Those reagents were used for validating experimental flotation tests. As a depressor, the blend of sodium pyrophosphate and sodium silicate was used with a fixed consumption rate of 200 g/t. As a collector, the emulsion of spindle oil and oxyethylated nonyl-phenol was used based on the theoretical research results. The consumption rate varied from 500 g/t to 1500 g/t.

The results of the flotation experiments are shown in Table 4.

Table 4. Results of coal flotation tests.

		Collector Consumption = 500 g/t							
Products	Yield, %	Content, %				Recovery, %			
		Ash	Si	Ca	S	Ash	Si	Ca	S
Concentrate	68.62	11.04	2.30	1.02	0.38	26.98	33.20	20.66	53.92
Tailings	31.38	65.34	10.12	8.57	0.51	73.02	66.80	79.34	46.08
Feed	100.00	28.08	4.75	3.39	0.42	100.00	100.00	100.00	100.00
		Collector Consumption = 1000 g/t							
Products	Yield, %	Content, %				Recovery, %			
		Ash	Si	Ca	S	Ash	Si	Ca	S
Concentrate	79.52	11.47	2.41	1.04	0.39	32.48	40.27	24.40	73.82
Tailings	20.48	92.57	13.86	12.51	0.54	67.52	59.73	75.60	26.18
Feed	100.00	28.08	4.75	3.39	0.42	100.00	100.00	100.00	100.00

Table 4. Cont.

Products	Yield, %	Collector Consumption = 1500 g/t							
		Content, %				Recovery, %			
		Ash	Si	Ca	S	Ash	Si	Ca	S
Concentrate	82.27	13.32	2.73	1.11	0.43	39.03	47.12	26.97	83.51
Tailings	17.73	96.57	14.18	13.96	0.39	60.97	52.88	73.03	16.49
Feed	100.00	28.08	4.75	3.39	0.42	100.00	100.00	100.00	100.00

Obtained results confirmed the hypothesis of collector and depressor action in flotation. Adding a mixture of depressor ash content decreases the concentrate by 5.09% at a lower collector consumption of 500 g/t. However, the yield of concentrate decreases by 8.61%. When the collector consumption rate is increased to 1000 g/t, the concentrate yield increases to 79.52% with a slight increase in ash content of 0.43%. When the collector consumption rate is increased to 1500 g/t, the concentrate yield and ash content increase by 2.75% and 1.85%, respectively, relative to the 1000 g/t flow rate. Moreover, at an increased flow rate of up to 1500 g/t, there is an increase in sulfur of 0.1% in relation to the flow rate of 500 g/t, which causes a harmful impurity upon further coal processing.

Based on the interpretation of the obtained results, it can be concluded that the collector flow rate of 1000 g/t is sufficient to obtain relatively high performance in coal flotation when using a mixture of depressors consisting of sodium silicate and sodium pyrophosphate.

4. Conclusions

The retrofitting of the coal flotation reagent mode is possible due to comprehensive studies of the kinetics of surface processes during coal flotation as well as the obtainment of new thermodynamic and kinetic parameters for the numerical characterization of flotation separation processes on the basis of numerical simulation.

The analysis of surface free energy and its components' calculation results for the coal surface during its treatment with n-hexane showed the possibility of the apolar reagent microdroplet formation on the coal surface, which has a higher potential for the formation of bonds of a dispersive nature. The results obtained prove the necessity of providing the contact time at which the formation of reagent microdroplets adsorbed from the liquid phase will occur.

For a more detailed study of the peculiarities of the mechanisms of fixation of reagents on the coal surface and their influence on the separation efficiency, methods of quantum-chemical modeling of coal-adsorbate systems and the potentiometric study of interfacial characteristics are proposed. On the basis of molecular modeling, it is established that the joint application of n-hexane and phenol leads to a synergetic effect of increasing the efficiency of reagents' fixation on the molecular fragment of the coal surface. This allowed us to predict the possible effectiveness of a collector with aromatic and aliphatic functional groups. This hypothesis was tested for the oxyethylated nonyl-phenol. Quantum-chemical modeling showed the high probability of physisorption, as the decrease in the energy of the system was 0.05562 eV. According to the results of potentiometric studies of interfacial characteristics, it was found that for the studied values of the flow rate of oxyethylated nonyl-phenol, the highest value of the E_f criterion was achieved at a reagent sorption value of 63.99% of the limiting sorption capacity, which shows the efficient hydrophobization of the coal surface.

An experimental validation of the hydrophobizing properties of the three depressors was carried out. The highest efficiency was found for spindle oil against coal. The hydrophilizing properties of three depressor reagents were investigated. The highest effi-

ciency was established for sodium pyrophosphate in relation to quartz and calcite. Based on the results of the interfacial characteristics study in the previous sections, for test flotation, the blend of sodium pyrophosphate and sodium silicate was used as a depressor, and the emulsion of spindle oil and oxyethylated nonyl-phenol was used as a collector. The proposed flotation reagents allowed us to achieve 26.98% ash recovery in the concentrate.

Author Contributions: Conceptualization, T.N.A.; methodology, T.N.A. and V.V.K.; software, V.V.K.; validation, T.N.A. and V.V.K.; formal analysis, T.N.A. and V.V.K.; investigation, V.V.K. and E.O.P.; writing—original draft preparation, T.N.A. and V.V.K.; writing—review and editing, T.N.A. and V.V.K.; visualization, V.V.K.; supervision, T.N.A. All authors have read and agreed to the published version of the manuscript.

Funding: This work was carried out with a grant from the Russian Science Foundation (Project N 23-47-00109).

Data Availability Statement: The original contributions presented in the study are included in the article; further inquiries can be directed to the corresponding author.

Conflicts of Interest: The authors declare no conflicts of interest.

References

1. BP Statistical Review of World Energy Statistical Review of World Energy. Available online: <https://www.bp.com/en/global/corporate/energy-economics/statistical-review-of-world-energy.html> (accessed on 12 December 2024).
2. Dvoynikov, M.V.; Leusheva, E.L. Modern trends in hydrocarbon resources development. *J. Min. Inst.* **2022**, *258*, 879–880.
3. Blinova, E.; Ponomareko, T.; Tesovskaya, S. Key Corporate Sustainability Assessment Methods for Coal Companies. *Sustainability* **2023**, *15*, 5763. [CrossRef]
4. Chanturia, V.A.; Shadrinova, I.V.; Gorlova, O.E. Innovative processes of deep and environmentally safe processing of technogenic raw materials in the conditions of new economic challenges. *Sustain. Dev. Mt. Territ.* **2021**, *13*, 224–237. [CrossRef]
5. Zhao, Y.; Yang, X.; Luo, Z.; Duan, C.; Song, S. Progress in developments of dry coal beneficiation. *Int. J. Coal Sci. Technol.* **2014**, *1*, 103–112. [CrossRef]
6. Hughes, N.; le Roux, M.; Campbell, Q.P.; Nakhaei, F. A review of the dry methods available for coal beneficiation. *Miner. Eng.* **2024**, *216*, 108847. [CrossRef]
7. Bazhin, V.Y.; Kuskov, V.B.; Kuskova, Y.V. Processing of low-demand coal and other carbon-containing materials for energy production purposes. *Inżynieria Miner.* **2019**, *21*, 195–198. [CrossRef]
8. Zubov, V.P.; Golubev, D.D. Prospects for the use of modern technological solutions in the flat-lying coal seams development, taking into account the danger of the formation of the places of its spontaneous combustion. *J. Min. Inst.* **2021**, *250*, 534–541. [CrossRef]
9. Karmakar, A.; Gopinathan, P.; Kumar, O.P.; Sethi, M.K.; Subramani, T.; Santosh, M.; Banerjee, P.K. Transformation in energy content of non-coking coals during differential settling beneficiation process: Implications for energy impact. *Fuel* **2024**, *377*, 132662. [CrossRef]
10. Vasilenko, T.; Kirillov, A.; Islamov, A.; Doroshkevich, A.; Ludzik, K.; Chudoba, D.M.; Mita, C. Permeability of a coal seam with respect to fractal features of pore space of fossil coals. *Fuel* **2022**, *329*, 125113. [CrossRef]
11. Chukaeva, M.A.; Matveeva, V.A.; Sverchkov, I.P. Complex processing of high-carbon ash and slag waste. *J. Min. Inst.* **2022**, *253*, 97–104. [CrossRef]
12. Aleksandrova, T.; Nikolaeva, N.; Afanasova, A.; Chenlong, D.; Romashev, A.; Aburova, V.; Prokhorova, E. Increase in Recovery Efficiency of Iron-Containing Components from Ash and Slag Material (Coal Combustion Waste) by Magnetic Separation. *Minerals* **2024**, *14*, 136. [CrossRef]
13. Tsareva, A.A.; Litvinova, T.E.; Gapanyuk, D.I.; Rode, L.S.; Poltoratskaya, M.E. Kinetic Calculation of Sorption of Ethyl Alcohol on Carbon Materials. *Russ. J. Phys. Chem. A* **2024**, *98*, 421–430. [CrossRef]
14. Kondratev, S.A.; Khamzina, T.A. Improvement of concentrate quality in flotation of low-rank coal. *J. Min. Inst.* **2024**, *265*, 65–77.
15. Aleksandrova, T.N.; Kuskov, V.B.; Afanasova, A.V.; Kuznetsov, V.V. Improvement of the fine coking coal flotation technology. *Obogashchenie Rud* **2021**, *3*, 9–13. [CrossRef]
16. Mao, Y.; Shen, P.; Dong, L.; Yu, X.; Xie, G.; Li, Y.; Liu, D. Role of oil droplet size on dynamic pore wetting of active carbon and particle-bubble interaction: New inspiration for enhancing the porous mineral floatability. *Colloids Surf. A Physicochem. Eng. Asp.* **2024**, *698*, 134611. [CrossRef]
17. Cheng, G.; Zhang, M.; Lu, Y.; Zhang, H.; Von Lau, E. New insights for improving low-rank coal flotation performance via emulsified waste fried oil collector. *Fuel* **2024**, *357*, 129925. [CrossRef]

18. Zhang, R.; Xing, Y.; Xia, Y.; Guo, F.; Ding, S.; Tan, J.; Gui, X. Synergistic adsorption mechanism of anionic and cationic surfactant mixtures on low-rank coal flotation. *ACS Omega* **2020**, *5*, 20630–20637. [CrossRef]
19. Chen, S.; Yang, Z.; Chen, L.; Tao, X.; Tang, L.; He, H. Wetting thermodynamics of low rank coal and attachment in flotation. *Fuel* **2017**, *207*, 214–225. [CrossRef]
20. Tian, Q.; Wang, H.; Pan, Y. Associations of gangue minerals in coal flotation tailing and their transportation behaviors in the flotation process. *ACS Omega* **2022**, *7*, 27542–27549. [CrossRef]
21. Petrakov, D.G.; Loseva, A.V.; Alikhanov, N.T.; Jafarpour, H. Standards for selection of surfactant compositions used in completion and stimulation fluids. *Int. J. Eng.* **2023**, *36*, 1605–1610. [CrossRef]
22. Niu, C.; Xia, W.; Peng, Y. Analysis of coal wettability by inverse gas chromatography and its guidance for coal flotation. *Fuel* **2018**, *228*, 290–296. [CrossRef]
23. Fuerstenau, D.W.; Rosenbaum, J.M.; Laskowski, J. Effect of surface functional groups on the flotation of coal. *Colloids Surf.* **1983**, *8*, 153–173. [CrossRef]
24. Kadagala, M.R.; Nikkam, S.; Tripathy, S.K. A review on flotation of coal using mixed reagent systems. *Miner. Eng.* **2021**, *173*, 107217. [CrossRef]
25. Xia, Y.; Zhang, R.; Cao, Y.; Xing, Y.; Gui, X. Role of molecular simulation in understanding the mechanism of low-rank coal flotation: A review. *Fuel* **2020**, *262*, 116535. [CrossRef]
26. Huang, J.; Li, Z.; Chen, B.; Cui, S.; Lu, Z.; Dai, W.; Zhao, Y.; Duan, C.; Dong, L. Rapid detection of coal ash based on machine learning and X-ray fluorescence. *J. Min. Inst.* **2022**, *256*, 663–676. [CrossRef]
27. Lian, F.; Li, G.; Cao, Y.; Zhao, B.; Zhu, G.; Fan, K. Experimental study on the dispersion behavior of a microemulsion collector and its mechanism for enhancing low-rank coal flotation. *Int. J. Min. Sci. Technol.* **2023**, *33*, 893–901. [CrossRef]
28. Xia, W.; Li, Y.; Nguyen, A.V. Improving coal flotation using the mixture of candle soot and hydrocarbon oil as a novel flotation collector. *J. Clean. Prod.* **2018**, *195*, 1183–1189. [CrossRef]
29. Rudolph, M.; Hartmann, R. Specific surface free energy component distributions and flotabilities of mineral microparticles in flotation—An inverse gas chromatography study. *Colloids Surf. A Physicochem. Eng. Asp.* **2017**, *513*, 380–388. [CrossRef]
30. Zhu, X.; Wei, H.; Hou, M.; Wang, Q.; You, X.; Li, L. Thermodynamic behavior and flotation kinetics of an ionic liquid microemulsion collector for coal flotation. *Fuel* **2020**, *262*, 116627. [CrossRef]
31. Han, H.; Liu, A.; Wang, C.; Yang, R.; Li, S.; Wang, H. Flotation kinetics performance of different coal size fractions with nanobubbles. *Int. J. Miner. Metall. Mater.* **2022**, *29*, 1502–1510. [CrossRef]
32. Avogadro: An Open-Source Molecular Builder and Visualization Tool. Version 1.XX. Available online: <http://avogadro.cc/> (accessed on 9 January 2025).
33. Hanwell, M.D.; Curtis, D.E.; Lonie, D.C.; Vandermeersch, T.; Zurek, E.; Hutchison, G.R. Avogadro: An advanced semantic chemical editor, visualization, and analysis platform. *J. Cheminform.* **2012**, *4*, 17. [CrossRef]
34. Snyder, H.D.; Kucukkal, T.G. Computational chemistry activities with Avogadro and ORCA. *J. Chem. Educ.* **2021**, *98*, 1335–1341. [CrossRef]
35. Neese, F. Software update: The ORCA program system, version 4.0. *Wiley Interdiscip. Rev. Comput. Mol. Sci.* **2018**, *8*, e1327. [CrossRef]
36. Takano, Y.; Houk, K.N. Benchmarking the conductor-like polarizable continuum model (CPCM) for aqueous solvation free energies of neutral and ionic organic molecules. *J. Chem. Theory Comput.* **2005**, *1*, 70–77. [CrossRef] [PubMed]
37. Owens, D.K.; Wendt, R.C. Estimation of the surface free energy of polymers. *J. Appl. Polym. Sci.* **1969**, *13*, 1741–1747. [CrossRef]
38. Usui, S.; Sasaki, H.; Matsukawa, H. The dependence of zeta potential on bubble size as determined by the dorn effect. *J. Colloid Interface Sci.* **1981**, *81*, 80–84. [CrossRef]
39. Booth, F. Sedimentation potential and velocity of solid spherical particles. *J. Chem. Phys.* **1954**, *22*, 1956–1968. [CrossRef]
40. Langmuir, I. The mechanism of the surface phenomena of flotation. *Trans. Faraday Soc.* **1920**, *15*, 62–74. [CrossRef]
41. Laskowski, J.S. Thermodynamic and kinetic flotation criteria. *Miner. Processing Extr. Metall. Rev.* **1989**, *5*, 25–41. [CrossRef]
42. Mohammadi-Jam, S.; Burnett, D.J.; Waters, K.E. Surface energy of minerals—Applications to flotation. *Miner. Eng.* **2014**, *66*, 112–118. [CrossRef]
43. Janczuk, B.; Wojcik, W.; Bialopiotrowicz, T. Wettability of coal surface and its surface free energy components. *Croat. Chem. Acta* **1988**, *61*, 51–63.
44. Marzec, A. Macromolecular and molecular model of coal structure. *Fuel Process. Technol.* **1986**, *14*, 39–46. [CrossRef]
45. Zhang, Z.; Wang, C.; Yan, K. Adsorption of collectors on model surface of Wiser bituminous coal: A molecular dynamics simulation study. *Miner. Eng.* **2015**, *79*, 31–39. [CrossRef]

Disclaimer/Publisher’s Note: The statements, opinions and data contained in all publications are solely those of the individual author(s) and contributor(s) and not of MDPI and/or the editor(s). MDPI and/or the editor(s) disclaim responsibility for any injury to people or property resulting from any ideas, methods, instructions or products referred to in the content.